Available online at www.sciencedirect.com
SCIENCE DIRECT®
Phytochemistry 66 (2005) 277–284
PHYTOCHEMISTRY
www.elsevier.com/locate/phytochem

Starter substrate specificities of wild-type and mutant polyketide synthases from Rutaceae

Richard Lukačin [a,1], Stephan Schreiner [a,1], Katrin Silber [b], Ulrich Matern [a,*]

[a] *Institut für Pharmazeutische Biologie, Philipps-Universität Marburg, Deutschhausstrasse 17 A, D-35037 Marburg, Germany*
[b] *Institut für Pharmazeutische Chemie, Philipps-Universität Marburg, Marbacher Weg 6, D-35032 Marburg, Germany*

Received 29 September 2004; received in revised form 29 November 2004

Abstract

Chalcone synthases (CHSs) and acridone synthases (ACSs) belong to the superfamily of type III polyketide synthases (PKSs) and condense the starter substrate 4-coumaroyl-CoA or *N*-methylanthraniloyl-CoA with three malonyl-CoAs to produce flavonoids and acridone alkaloids, respectively. ACSs which have been cloned exclusively from *Ruta graveolens* share about 75–85% polypeptide sequence homology with CHSs from other plant families, while 90% similarity was observed with CHSs from Rutaceae, i.e., *R. graveolens*, *Citrus sinensis* and *Dictamnus albus*. CHSs cloned from many plants do not accept *N*-methylanthraniloyl-CoA as a starter substrate, whereas ACSs were shown to possess some side activity with 4-coumaroyl-CoA. The transformation of an ACS to a functional CHS with 10% residual ACS activity was accomplished previously by substitution of three amino acids through the corresponding residues from *Ruta*-CHS1 (Ser132Thr, Ala133Ser and Val265Phe). Therefore, the reverse triple mutation of *Ruta*-CHS1 (mutant R2) was generated, which affected only insignificantly the CHS activity and did not confer ACS activity. However, competitive inhibition of CHS activity by *N*-methylanthraniloyl-CoA was observed for the mutant in contrast to wild-type CHSs. Homology modeling of ACS2 with docking of 1,3-dihydroxy-*N*-methylacridone suggested that the starter substrates for CHS or ACS reaction are placed in different topographies in the active site pocket. Additional site specific substitutions (Asp205Pro/Thr206Asp/His207Ala or Arg60Thr and Val100Ala/Gly218Ala, respectively) diminished the CHS activity to 75–50% of the wild-type CHS1 without promoting ACS activity. The results suggest that conformational changes in the periphery beyond the active site cavity volumes determine the product formation by ACSs vs. CHSs in *R. graveolens*. It is likely that ACS has evolved from CHS, but the sole enlargement of the active site pocket as in CHS1 mutant R2 is insufficient to explain this process.

Keywords: *Ruta graveolens* L; *Dictamnus albus*; Rutaceaee; Acridone synthase; Chalcone synthase; Site-directed mutagenesis

1. Introduction

Plant type III-polyketide synthases have recently been the object of numerous mutational studies. These enzymes condense a CoA-ester starter substrate with malonyl-CoA(s) to a linear polyketide intermediate which is properly folded for cyclization to the final product. The choice of starter substrate, the number of condensations and the particular type of folding are in the focus of the investigations. Chalcone synthase (CHS), stilbene synthase (STS) and acridone synthase (ACS) catalyze three steps of condensation and produce tetraketide intermediates from the starter substrate 4-coumaroyl-CoA or *N*-methylanthraniloyl-CoA (Fig. 1). CHS, ACS and STS are closely related enzymes as

Abbreviations: ACS, acridone synthase; CHS, chalcone synthase; PKS, polyketide synthase; STS, stilbene synthase; DMA, 1,3-dihydroxy-*N*-methylacridone

* Corresponding author. Tel.: +49 6421 282 2461; fax +49 6421 282 6678.
E-mail address: matern@staff.uni-marburg.de (U. Matern).

[1] These authors contributed equally to the work presented.

0031-9422/$ - see front matter © 2004 Elsevier Ltd. All rights reserved.
doi:10.1016/j.phytochem.2004.11.023

shown by immunological cross reactivities, superimposible CD-spectra and by molecular modeling studies (Lukačin et al., 2001; Austin and Noel, 2003), although their polypeptide sequences may differ by about 100 residues at an overall length of about 390 residues (Austin and Noel, 2003). STS has presumably evolved independently more than once from CHS, as was demonstrated in *Pinus sylvestris* or *Arachis hypogaea* (Tropf et al., 1994). Thus, CHS and STS follow different modes of folding of the same intermediate, but the structural cause of divergence still remains to be solved. ACS accomplishes yet another type of folding (Fig. 1) and, in addition, uses a different starter substrate. While CHSs and, to a lesser extent, STSs are widely distributed in spermatophytes, ACSs appear to be confined to the Rutaceae family. Two ACSs have been cloned from *Ruta graveolens*, and it is noteworthy that the recombinant enzymes possess CHS side activity in the order of 15–20%, in contrast to all known CHSs which literally do not show ACS activity. It is likely that ACS has also evolved from CHS.

Insight into the catalytic mechanism of CHS has been significantly advanced by the X-ray diffraction of crystallized CHS from *Medicago sativa* (Ferrer et al., 1999) and of 2-pyrone synthase from *Gerbera* (Jez et al., 2000a,b). In context with site-directed mutagenesis this identified the active site amino acid residues which include a cysteine serving as a nucleophile in the condensing reaction and, in case of CHS, further three residues (Phe215, His303 and Asn336) shown to be involved in the binding and decarboxylation of malonyl-CoA concomitantly with the condensing reaction (Ferrer et al., 1999; Jez et al., 2000a,b). The strict conservation of these residues in the sequences of CHS, STS and ACS implies an analogous reaction mechanism for these enzymes (Jez et al., 2000b). It is noteworthy, that benzalacetone synthase which catalyses the condensation of the starter substrate 4-coumaroyl-CoA with a single malonyl-CoA lacks the active site Phe215 (numbering as in *M. sativa* CHS), and the mutation Phe215Ser of *Medicago* CHS generated a novel CHS capable of accepting also *N*-methylanthraniloyl-CoA as a starter substrate

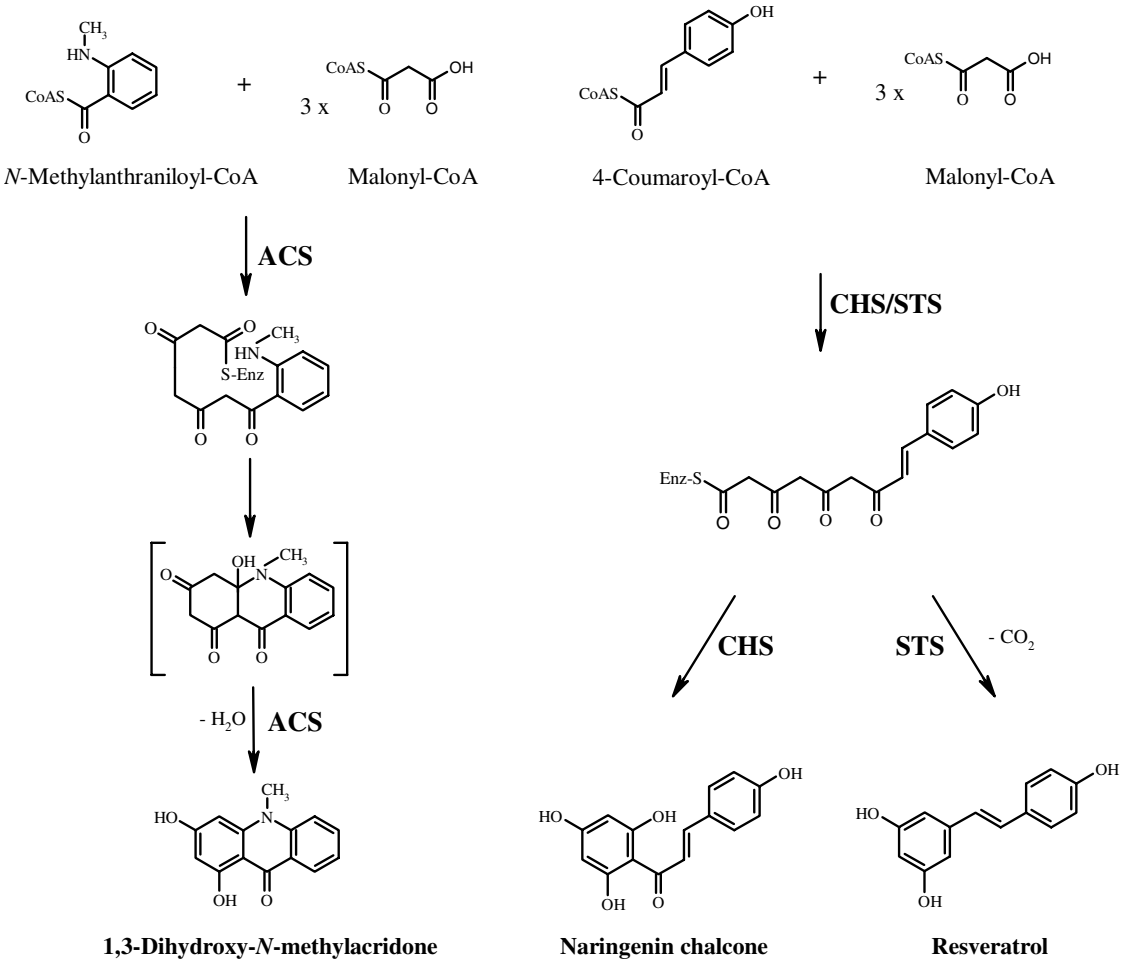

Fig. 1. Reactions catalysed by ACS, CHS or STS. Claisen-type cyclization leads to the formation of naringenin chalcone, while an aldol-type cyclization concomitant with decarboxylation produces *trans*-3,4′,5-trihydroxystilbene (resveratrol). The nucleophilic substitution followed by dehydration appears to be required for the cyclization to 1,3-dihydroxy-*N*-methylacridone.

(Jez et al., 2002). Nevertheless, unnatural *N*-methylanthraniloyltriacetic acid lactone resulted from this side activity probably by spontaneous lactonization of the linear tetraketide intermediate. Very recently STS was also crystallized, and a conformational change of the main chain induced by a peculiar short, buried loop that spans the two active sites (residues 132–137) in the dimer interface (Austin and Noel, 2003) was proposed to be responsible for the alternate cyclization of the tetraketide intermediate.

In contrast to the differences between CHS and STS, the limited volume of the active site cavity in CHS was considered to be responsible for the lack of ACS activity (Jez et al., 2000a). However, the exclusion of the proper starter substrate has not been established experimentally. The opposite approach, replacing the active site cavity lining residues Ser132, Ala133 and Val265 in ACS by the more voluminous residues Thr, Ser and Phe as found in CHS, successfully transformed the ACS into a CHS with marginal ACS side activity (Lukačin et al., 2001). In this report the relevance of these three active site amino acid residues for starter substrate selectivity is examined in CHS1 from *R. graveolens*. Furthermore, molecular modeling and docking studies were employed to assign essential residues for mutation and to explain the crucial role of Val265 or Phe267 for ACS and CHS activity.

2. Results

2.1. Characterization of active sites in Ruta ACS mutants

The starter substrate preference of CHSs and related enzymes has been attributed, at least in part, to the geometry of the active site cavities, and the restriction of the initiation/elongation cavity volume converted alfalfa CHS to a functional 2-pyrone synthase (Jez et al., 2000a). Following this principle, the mutants MS3.1 (Val265Phe) and MS3.2 (Ser132Thr, Ala133Ser and Val265Phe) of ACS2 from *R. graveolens* were generated previously thereby demonstrating the transformation to CHS with marginal ACS side activity for the triple mutant (Lukačin et al., 2001). It must be emphasized that in these experiments all enzyme assays were conducted at 40 °C for optimal ACS activity rather than at 30 °C which is commonly used for the determination of CHS activity. Homology modeling based on the crystal structure of alfalfa CHS (Ferrer et al., 1999) and calculation with software CASTP (Liang et al., 1998) of the active site cavity volumes of wildtype-ACS2, mutant MS3.1 and mutant MS3.2 revealed 1100, 1060 and 1036 Å^3, respectively, the latter value being close to the cavity volume in alfalfa CHS (1019 Å^3). Docking of naringenin chalcone or 1,3-dihydroxy-*N*-methylacridone (DMA), the immediate products of CHS and ACS, respectively, into the wildtype-ACS2 model cavity unexpectedly assigned two energetically almost equivalent binding locations to either ligand in the homodimeric enzyme, and thus the folding and/or positioning of the condensation product appears feasible at two topological sites in ACS (Fig. 2). Binding of DMA as shown in yellow is possible in ACS, but not in CHS, because Phe replacing Val265 (Fig. 2) induces a conformation on the binding pocket in which the Phe ring interferes with the ligand. Moreover, the yellow depicted docking position likely represents the preferred binding site, because it is located close to the CoA-binding tunnel as the sole exit from the enzyme dimer. The results might explain the CHS side activity of ACSs and the lack of ACS side activity in wildtype CHSs.

Although several rotamers of Phe265 seemed possible, model calculations for the enzymes hosting a product (DMA or naringenin chalcone) consistently defined a spatial configuration of the Phe ring (Fig. 2) quite different from that in the unloaded enzymes. Obviously, the energy constraints of ligand binding require a less favourable orientation of Phe265, whereas without this limitation (deliberate choice of Phe265 rotamer) or, for example, replacement of Phe265 by Val, the CHS model would provide the active site space to accommodate also DMA. Nevertheless, CHSs generally lack ACS activity in support of the docking studies, and the exact

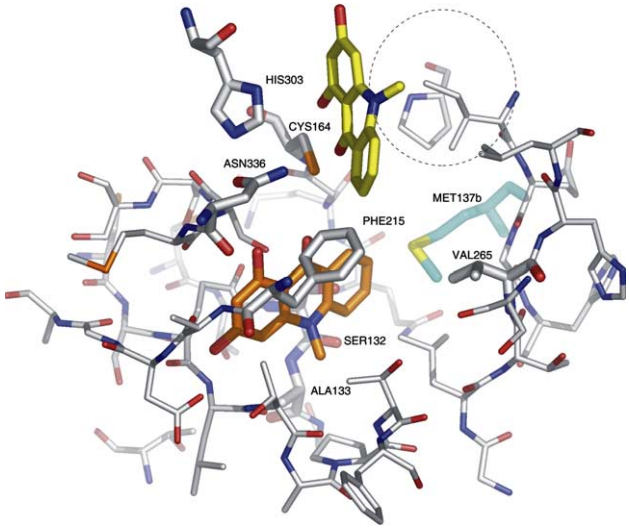

Fig. 2. Docking of 1,3-dihydroxy-*N*-methylacridone (DMA) into the active site of homodimeric *Ruta* ACS2. The active site view is shown along the perspective from the CoA-binding tunnel (indicated by the broken circle), and the single residue per monomer interacting with the opposing subunit (Met137) as well as the residues of the catalytic triad (Cys164, His303, Asn336) are marked. Residue Gly211 was omitted for clarity. Two docking solutions for DMA of nearly equal ranking (shown in yellow, close to the CoA-binding tunnel exit, and orange) were calculated. The residues most relevant for the active site cavity volume (Ser132, Ala133, Val265) are designated. The figure was prepared using PyMol (http://www.pymol.org).

mechanism forming the rigid acridone ring system remains to be established. In contrast, ACS is still capable of forming some conformationally flexible naringenin chalcone. It is conceivable that, beyond the volume of the activity site cavity, long range adjustments of the enzyme backbone affect the ACS activity, which should eventually be unraveled from crystallisation studies (ongoing collaboration with J.P. Noel, San Diego, USA).

2.2. Specificities of Ruta CHS mutants

In a reverse approach, the corresponding residues were substituted in CHS1 from *R. graveolens* (Springob et al., 2000), generating the single-site mutant R1 (Phe267Val) and the triple mutant R2 (Thr134Ser, Ser135Ala and Phe267Val), and the recombinant enzymes were examined at 30 °C for CHS or ACS activity in comparison to the wild-type *Ruta*-CHS. Neither mutation affected the CHS activity to a significant extent (Table 1), and no ACS activity was observed under these conditions. When the assays were repeated at 40 °C, however, low level ACS activity (approx. 3% of wild-type CHS, assayed at 30 °C) was determined with the mutant R1, whereas the mutant R2 was inactive under these conditions (Table 1). Therefore, the activities of the previously generated ACS2 mutants MS3.1 and MS3.2 were re-examined at 30 °C and revealed a puzzling effect of temperature on the MS3.2 mutant only. This mutant which represents a functional CHS, nonetheless possessing some ACS side activity in contrast to all wild-type CHSs (Lukačin et al., 2001; Austin and Noel, 2003), showed 2.3-fold higher specific CHS activity at 40 °C as compared to 30 °C.

The sequence of *Ruta*-CHS1 is about 75% homologous to that of alfalfa CHS (Springob et al., 2000), and a very similar spatial structure was generated for CHS1 by homology modeling. Comparison of the structural model with that of wild-type ACS2 assigned a few additional residues which might affect the CHS or ACS activity. These include Arg60 which lines the entrance of the CoA-binding tunnel in *Ruta*-CHS and is replaced by Thr in *Ruta*-ACS (Lukačin et al., 2001; Austin and Noel, 2003). Furthermore, Gly218 adjacent to the "gatekeeper" Phe217 (Austin and Noel, 2003; Jez et al., 2002) and Val100 are conserved in all plant type III PKSs (Austin and Noel, 2003) except for ACSs encoding Ala in these positions (Fig. 3). Three further mutants were therefore created from CHS1 mutant R2 (Fig. 3) carrying the additional substitutions Asp205Pro, Thr206Asp, His207Ala (mutant R3) or Arg60Thr (mutant R4) and Val100Ala, Gly218Ala (mutant R5). Western blotting confirmed that the soluble recombinant enzymes were expressed in *Escherichia coli* at equivalent rates. The mutations reduced the specific CHS activity by about 20–50% in comparison to wild-type CHS1 (Table 1). Finally, additional four mutations (Asn87Glu, Ala90Lys, Gln240Tyr and Ala361Ser) were introduced in mutant R5, in analogy to the sequence of *Dictamnus* CHS (see below), to yield mutant R6 which did not suppress the CHS activity any further. However, these mutants did not develop ACS activity, and the amino acid substitution in R1 through R6 are not crucial for CHS product formation but reduce the turnover rate.

Table 1
CHS activities of wild-type and mutant *Ruta* CHSs[a]

Enzyme	Relative activity (%)	
	30 °C	40 °C
Wildtype-CHS	100	99
R1 (F267V)	47	56
R2 (T134S, S135A, F267V)	83	64
R3 (T134S, S135A, F267V, D205P, T206D, H207A)	53	65
R4 (T134S, S135A, F267V, R60T)	57	56
R5 (T134S, S135A, F267V, V100A, G218A)	52	76

[a] All enzyme activities relate to the CHS activity of the wild-type CHS at 30 °C (100%). No ACS activity was detected in assays conducted at 30 °C, but approximately 3% ACS activity was measured for mutant R1 assayed at 40 °C.

2.3. Cloning and specificity of Dictamnus CHS

The reliable comparison of polyketide synthases using *N*-methylanthraniloyl-CoA or 4-coumaroyl-CoA as the starter substrate requires the analysis of enzymes from more than one plant. CHSs had been cloned from only two species of the Rutaceae, *R. graveolens* and *Citrus* (Springob et al., 2000; Moriguchi et al., 1999), and the anthranilate secondary metabolism of *Citrus* has not been thoroughly studied. We therefore initiated the cloning of polyketide synthases from *Dictamnus albus* known to accumulate predominantly furoquinoline alkaloids from anthraniloyl-CoA and malonyl-CoA (Dewick, 2002). As the first example, CHS was cloned by RT-PCR using degenerate oligonucleotide primers. The full length cDNA of 1173 bp encoded a polypeptide of 42.7 kDa (Fig. 3) that was expressed with a His-tag in *E. coli* and purified to homogeneity (Fig. 4). The pure enzyme exhibited CHS activity in the order of 20 μkat/kg without even a trace of ACS activity when assayed at 30 or 40 °C. The alignment of the polypeptide with those of CHSs and ACSs from *R. graveolens* revealed a high degree of identity (about 93%) with a few exchanges in comparison to the ACS sequence (Fig. 3) which might be considered as a lead to further mutations.

2.4. Starter substrate affinity of CHSs

The observation that *Ruta*-CHS1 mutant R1 developed marginal ACS activity under particular conditions

```
CHSruta     MAAVTVEAIRKAQRADGPAAVLAIGTATPANYVTQADYPDYYFRITKSEHMTELKEKFKR 60
CHSdict     --MATVEEIIKAKRAEGPATILAIGTATPANSVNQADYPDYYFRITKSEHMTELKEKFKR 58
CHScitr     --MATVQEIRNAQRADGPATVLAIGTATPAHSVNQADYPDYYFRITKSEHMTELKEKFKR 58
ACSruta     --MESLKEMRKAQKSEGPAAILAIGTATPDNVYIQADYPDYYFKIT-SEHMTELKDKFKT 57
                ***  * ******************  *   ************ ************

CHSruta     MCDKSMIRKRYMHLTEDILKENPNMCAYMAPSLDARQDIVVVEVPKLGKEAAVKAIKEWG 120
CHSdict     MCDKSMIKKRYMHLTEDILKENPNMCAYMAPSLDARQDVVVVEVPKLGKEAATKAIKEWG 118
CHScitr     MCDKSMIKKRYMYLTEEILKENPNMCAYMAPSLDARQDIVVVEVPKLGKEAATKAIKEWG 118
ACSruta     LCEKSMIRKRHMCFSQEFLKANPEVCKHMGKSLNARQDIAVVETPRIGKEAAVKAIKEWG 117
            ************ ******* ***** **  ******** *** ******** *******

CHSruta     QPKSKITHLIFCTTSGVDMPGCDYQLTKLLGLRPSVKRFMMYQQGCFAGGTVLRLAKDLA 180
CHSdict     QPKSKITHLVFCTTSGVDMPGADYQLTKLLGLRPSVKRLMMYQQGCFAGGTVLRLAKDLA 178
CHScitr     QPKSKITHLIFCTTSGVDMPGADYQLTKLIGLRPSVKRFMMYQQGCFAGGTVLRLAKDLA 178
ACSruta     HPKSSITHLIFCTSAGVDMPGADYQLTRMLGLNPSVKRMMIYQQGCYAGGTVLRLAKDLA 177
            **** ***************** ********** ***************************

CHSruta     ENNRGARVLVVCSEITAVTFRGPADTHLDSLVGQALFGDGAAAVIVGADPDESIERPLYQ 240
CHSdict     ENNKGARVLVVCSEITAVTFRGPADTHLDSLVGQALFGDGAAALIVGADPDTTVERPLYQ 238
CHScitr     ENNKGARVLVVCSEITAVTFRGPADTHLDSLVGQALFGDGAAAVIVGADPDTSVERPLYQ 238
ACSruta     ENNKGSRVLVVCSELTAPTFRGPSPDAVDSLVGQALFADGAAALVVGADPDTSVERALYY 237
            ***************** ******   ********** ************* **** **

CHSruta     LVSAAQTILPDSDGAIDGHLREVGLTFHLLKDVPGLISKNIEKSLKEAFGPIGISDWNSI 300
CHSdict     LVSASQTILPDSDGAIDGHLREVGLTFHLLKDVPGLISKNIEKSLVEAFSPIGINDWNSI 298
CHScitr     LVSTSQTILPDSDGAIDGHLREVGLTFHLLKDVPGLISKNIEKSLSEAFAPLGISDWNSI 298
ACSruta     IVSASQMLLPDSDGAIEGHIREEGLTVHLKKDVPALFSANIDTPLVEAFRPLGISDWNSI 297
            ****** *************** *** ** **** *** ***  * *** **** *****

CHSruta     FWIAHPGGPAILDQVEAKLGLKEEKLRATRQVLSEYGNMSSACVLFILDEMRKNCAEEGR 360
CHSdict     FWIAHPGGPAILDQVEEKLGLKEEKLRATRHVLSEYGNMSSACVLFILDEMRKKCVEEGK 358
CHScitr     FWIAHPGGPAILDQVESKLGLKGEKLKATRQVLSEYGNMSSACVLFILDEMRKKSVEEAK 358
ACSruta     FWIAHPGGPAILDQIEVKLGLKEDKLRASKHVMSEYGNMSSSCVLFVLDEMRNKSLQDGK 357
            *************** ***** ******************************  ** *

CHSruta     ATTGEGLDWGVLFGFGPGLTVETVVLRSVPIKA 393
CHSdict     ATTGEGLDWGVLFGFGPGLTVETVVLHSVPIKP 391
CHScitr     ATTGEGLDWGVLFGFGPGLTVETVVLHSVPIKA 391
ACSruta     STTGEGLDWGVLFGFGPGLTVETVVLRSVPVEA 390
            *********************************
```

Fig. 3. Alignment of *Ruta* CHS1, *Dictamnus* CHS, *Citrus* CHS and *Ruta* ACS2 polypeptides. Asterisks assign identical amino acids or conservative exchanges. The residues replaced by site-directed mutagenesis are marked by shading. The active site catalytic triad residues (Cys164, His303 and Asn336, numbering refers to CHS2 from *Medicago sativa*) is bold printed and underlined.

of incubation suggested that the Phe267Val exchange in CHSs is sufficient to promote binding of the starter substrate *N*-methylanthraniloyl-CoA. Therefore, we conducted inhibition studies using the mutants R1 through R5 in CHS assays at 30 °C in the presence of varying concentrations of *N*-methylanthraniloyl-CoA. The CHS activity of each of the CHS1 mutants was inhibited as predicted, and the IC_{50} values of 5.6 μM (R1), 2.2 μM (R2), 2.5 μM (R3), 4.1 μM (R4) and 2.6 μM (R5), respectively, documented relatively high affinities. A similar effect was also reported recently for the alfalfa CHS Phe265Val mutant (Jez et al., 2002). In contrast to alfalfa, however, binding of the ACS starter substrate did not lead to a detectable product. For comparison, the effect of *N*-methylanthraniloyl-CoA on CHS activity was also examined with wild-type CHSs from *Ruta graveolens*, *D. albus* or *Pinus sylvestris*. The activity of these enzymes was not affected significantly by the ACS starter substrate over a broad range of concentrations (2–50 μM).

3. Discussion

The pronounced effect of temperature on the ACS or CHS activity of the triple mutant MS3.2 and the mutant R1, respectively, argues for the conformational adoption of the enzyme backbones during catalysis on top of the restraints of the active site cavity. Furthermore, subtle steric and electronic changes in the microenvironment presumably affect the binding of substrate. A similar conclusion was drawn recently for the differential modes of action of stilbene vs. chalcone synthases (Austin and Noel, 2003), which are most likely due to a short loop in the main chain periphery inducing particular conformational states upon the polypeptides. In this instance, the different enzyme conformations appear to result from the replacement of Val98 in CHS by an amino acid residue with bulky side-chain in STS with the consequence of causing a different folding pattern of the linear tetraketide substrate intermediate. The ACS2 from *R. graveolens* encodes alanine at the corresponding

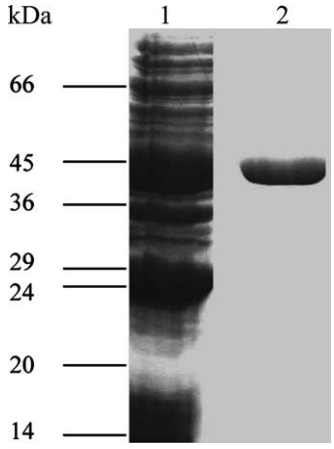

Fig. 4. SDS/PAGE separation of *Dictamnus* CHS expressed in *E. coli*. Crude bacterial extract (lane 1) was prepared in 50 mM sodium phosphate buffer pH 8.0, and the CHS was purified to homogeneity by Ni-NTA chromatography (lane 2). Separation was accomplished in 5% stacking and 12.5% separation gels followed by staining with Coomassie Brilliant Blue R250. Calibration by molecular mass markers is indicated in the left margin.

position (Ala100), which might be relevant for the cyclization step in the ACS reaction. The major hurdle for ACS activity, however, is the size and spatial configuration of the residue corresponding to Val265 (ACS2) or Phe267 (CHS1) (Fig. 2), because all CHS1 mutants, but none of the wild-type CHSs, bound the ACS starter substrate, and the mutant R1 even revealed weak ACS side activity under appropriate conditions. Residues Thr134 and Ser135 appear to be primarily important for CHS activity, because ACS2 mutants MS3.1 and MS3.2 differ marginally in their ACS activities, but showed greatly different CHS activities. This is supported by the CHS1 mutants, which in the 40 °C assays revealed minor ACS activity for mutant R1 and complete loss of activity for mutant R2. These data are compatible with the two topographic locations of 1,3-dihydroxy-*N*-methylacridone in ACS2 assigned by the docking experiments (Fig. 2). Ser132 and Ala133 line the site primarily binding naringenin chalcone and responsible for the CHS side activity, whereas Val265 is located at a different site of the active cavity and is possibly involved in the binding of *N*-methylanthraniloyl-CoA supporting ACS activity.

4. Experimental

4.1. Enzymes and materials

Biochemicals, vectors, *E. coli* host strains, restriction enzymes or DNA modifying enzymes were purchased from commercial companies as cited previously (Lukačin et al., 1999; Springob et al., 2000).

4.2. Structural CHS analysis and molecular modeling

Polypeptide sequence alignments were carried out with Clustal W (Thompson et al., 1994). Homology model of *Ruta* ACS (Fig. 2) was generated using MODELLER (Sali and Blundell, 1993) and alfalfa CHS (pdb-code 1CGK) as template structure (Ferrer et al., 1999). Subsequent docking runs were performed with the Lamarckian genetic algorithm included in AutoDock 3.0 (Morris et al., 1996) (standard parameters) and 10 independent runs per ligand. Polar hydrogens were added to proteins with the PROTONATE utility in AMBER 7 (Case et al., 2002). AMBER united-atom force-field charges (Weiner et al., 1984) were assigned, and solvation parameters were incorporated with the ADDSOL utility from AutoDock 3.0. For the ligands, Gasteiger partial atomic charges (Gasteiger and Marsili, 1980) were assigned, and free rotation of all bonds was provided. For both ligands, the optimal docking solution was chosen for the structure–activity comparison, and the relative binding affinity was predicted using the knowledge-based scoring function DrugScore (Gohlke et al., 2000).

4.3. CHS mutation

Based on the RgCHS I-pQE6 plasmid (Springob et al., 2000), the CHS mutants R1–R5 (Table 1) were generated by using the QuikChange® Multi Site-Directed Mutagenesis Kit (Stratagene, Amsterdam, The Netherlands) following the supplier's instructions and appropriate oligonucleotide primers (not shown). *E. coli* M15, harboring the plasmid pRep4, was transformed with the wild-type and mutant RgCHS I-pQE6 constructs, and the cells were propagated, induced for ACS expression and harvested as described previously (Lukačin et al., 1999, 2001). Crude bacterial extracts were prepared by ultrasonication, and the enzyme activities were assayed from the clear supernatant after centrifugation (30,000 *g*, 4 °C, 10 min). Equivalent rates of expression of the recombinant enzymes was confirmed by Western blotting.

4.4. Analytical methods

The activities of CHS and ACS were determined as reported previously (Lukačin et al., 1999, 2001). Protein amounts were determined according to Sandermann and Strominger (1972) with bovine serum albumin as a reference, and the protein composition of samples was examined by sodium dodecyl sulphate–polyacrylamide gel electrophoresis (SDS/PAGE) (Laemmli, 1970) and Western blotting (Towbin et al., 1979).

4.5. PCR cloning, expression and purification of *Dictamnus albus CHS*

Oligo(dT)-primed cDNA was synthesized from 5 μg total RNA isolated from *D. albus* roots and leaves in a 25 μl incubation using Superscript II reverse transcriptase (Life Technologies, Karlsruhe, Germany) and following the manufacturer's instruction. Degenerate primers designed from the CHS and ACS database accessions of *Citrus sinensis* and *R. graveolens* (forward: 5′-ATC AC(CT) AA(GC) AGC GAG CAC ATG AC-3′ and 5′-AAG GAC TTG GC(AGCT) GAG AAC AAC-3′; reverse: 5′-GGC CAC GCG TCG ACT AGT ACT TTT TTT TTT TTT TTT T-3′) were employed for PCR amplification. 5′-RACE was carried out with the GeneRacer™ Kit (Invitrogen, Groningen, The Netherlands) and employing a comercial forward primer and gene-specific primers deduced from isolated PCR fragments (5′-GAT GAG TAT CAG CGG GGC CAC G-3′, 5′-Acc GAA AAG AGC CTG CCC CAC G-3′). A full-size cDNA putatively encoding CHS was amplified. Subsequently, the cDNA was cloned into the T/A cloning bacterial expression vector pET101 (Invitrogen), the orientation was examined by DNA sequencing (Sanger et al., 1977) and the *E. coli* strain BL21 was transformed with the DaCHS1-pET101 expression construct, allowing the expression of DaCHS carrying an N-terminal His-tag. The expression of *Dictamnus* CHS was induced by the addition of isopropyl thio-β-D-galactoside (1 mM), and the bacteria were harvested as described elsewhere (Lukačin et al., 1999, 2001). Crude bacterial extracts were prepared by ultrasonification (Lukačin et al., 1999, 2001) and purification of the recombinant CHS were performed by affinity chromatography of the clear supernatant after centrifugation on a Ni-NTA agarose column (Qiagen, Hilden, Germany).

Note added in proof

After submission of this manuscript, the crystal structure of a pinosylvin-forming STS was reported in Chem. Biol. 11, 1179–1194, proposing the importance of electronic effects and an aldol switch for balancing the cyclization specificities in CHS and STS.

Acknowledgements

This work was supported by the Deutsche Forschungsgemeinschaft and Fonds der Chemischen Industrie. The authors appreciate the collaboration with Silvia Specker and Marc Hehmann on CHS cloning.

References

Austin, M.B., Noel, J.P., 2003. The chalcone synthase superfamily of type III polyketide synthases. Nat. Prod. Rep. 20, 79–110.

Case, D.A., Pearlman, D.A., Caldwell, J.W., Cheatham III, T.E., Wang, J., Ross, W.S., Simmerling, C.L., Darden, T.A., Merz, K.M., Stanton, R.V., Cheng, A.L., Vincent, J.J., Crowley, M., Tsui, V., Gohlke, H., Radmer, R.J., Duan, Y., Pitera, J., Massova, I., Seibel, G.L., Singh, U.C., Weiner, P.K., Kollman, P.A., 2002. AMBER 7. University of California, San Francisco.

Dewick, P.M., 2002. Medicinal Natural Products. A Biosynthetic Approach. Wiley, New York.

Ferrer, J.-L., Jez, J.M., Bowman, M.E., Dixon, R.A., Noel, J.P., 1999. Structure of chalcone synthase and the molecular basis of plant polyketide biosynthesis. Nat. Struct. Biol. 6, 775–784.

Gasteiger, J., Marsili, M., 1980. Iterative partial equalization of orbital electronegativity – a rapid access to atomic charges. Tetrahedron 36, 3219–3228.

Gohlke, H., Hendlich, M., Klebe, G., 2000. Knowledge-based scoring function to predict protein–ligand interactions. J. Mol. Biol. 295, 337–356.

Jez, J.M., Austin, M.B., Ferrer, J.-L., Bowman, M.E., Schröder, J., Noel, J.P., 2000a. Structural control of polyketide formation in plant-specific polyketide synthase. Chem. Biol. 7, 919–930.

Jez, J.M., Ferrer, J.-L., Bowman, M.E., Dixon, R.A., Noel, J.P., 2000b. Dissection of malonyl-coenzyme A decarboxylation from polyketide formation in the reaction mechanism of a plant polyketide synthase. Biochemistry 39, 890–902.

Jez, J.M., Bowman, M.E., Noel, J., 2002. Expanding the biosynthetic repertoire of plant type III polyketide synthases by altering starter molecule specificity. Proc. Natl. Acad. Sci. USA 99, 5319–5324.

Laemmli, U.K., 1970. Cleavage of structural proteins during the assembly of the head of bacterophage T4. Nature (London, UK) 227, 680–684.

Liang, J., Edelsbrunner, H., Woodward, C., 1998. Anatomy of protein pockets and cavities: measurement of binding site geometry and implications for ligand design. Protein Sci. 7, 1884–1897.

Lukačin, R., Springob, K., Urbanke, K., Ernwein, C., Schröder, G., Schröder, J., Matern, U., 1999. Native acridone synthases I and II from *Ruta graveolens* L. form homodimers. FEBS Lett. 448, 135–140.

Lukačin, R., Schreiner, S., Matern, U., 2001. Transformation of acridone synthase to chalcone synthase. FEBS Lett. 508, 413–417.

Moriguchi, T., Masayuki, K., Tomono, Y., Endo-Inagaki, T., Omura, M., 1999. One type of chalcone synthase gene expressed during embryogenesis regulates the flavonoid accumulation in *Citrus* cell cultures. Plant Cell Physiol. 40, 651–655.

Morris, G.M., Goodsell, D.S., Huey, R., Olson, A.J., 1996. Distributed automated docking of flexible ligands to proteins: parallel applications of AutoDock 2.4. J. Comput.-Aided Mol. Des. 10, 293–304.

Sali, A., Blundell, T.L., 1993. Comparative protein modelling by satisfaction of spatial restraints. J. Mol. Biol. 234, 779–815.

Sandermann Jr., H., Strominger, L., 1972. Purification and properties of C_{55}-isoprenoid alcohol phosphokinase from *Staphylococcus aureus*. J. Biol. Chem. 247, 5123–5131.

Sanger, F., Nicklen, S., Coulson, A.R., 1977. DNA sequencing with chain terminating inhibitors. Proc. Natl. Acad. Sci. USA 74, 5463–5467.

Springob, K., Lukačin, R., Ernwein, C., Gröning, I., Matern, U., 2000. Specificities of functionally expressed chalcone and acridone synthases from *Ruta graveolens*. Eur. J. Biochem. 267, 6552–6559.

Thompson, J.D., Higgins, D.G., Gibson, T.J., 1994. Clustal W: improving the sensitivity of progressive multiple sequence alignment through sequence weighting, position-specific gap penalties and weight matrix choice. Nucleic Acids Res. 22, 4673–4680.

Towbin, H., Staehlin, T., Gordon, J., 1979. Electrophoretic transfer of proteins from polyacrylamide gels to nitrocellulose sheets: procedure and some applications. Proc. Natl. Acad. Sci. USA 76, 4350–4354.

Tropf, S., Lanz, T., Rensing, S.A., Schröder, J., Schröder, G., 1994. Evidence that stilbene synthases have developed from chalcone synthases several times in the course of evolution. J. Mol. Evol. 38, 610–618.

Weiner, S.J., Kollman, P.A., Case, D.A., Singh, U.C., Ghio, C., Alagona, G., Profeta, S., Weiner, P., 1984. A new force field for molecular mechanical simulation of nucleic acids and proteins. J. Am. Chem. Soc. 106, 765–784.